

HMF: A Hybrid Multi-Factor Framework for Dynamic Intraoperative Hypotension Prediction

Mingyue Cheng¹, Jintao Zhang¹, Zhiding Liu¹, Chunli Liu^{2*}, Yanhu Xie³

¹State Key Laboratory of Cognitive Intelligence, University of Science and Technology of China

²Hefei University of Technology

³The First Affiliated Hospital of University of Science and Technology of China

mycheng@ustc.edu.cn, {zjt, zhiding}@mail.ustc.edu.cn, liuchunli@hfut.edu.cn, xyh200701@sina.cn

Abstract

Intraoperative hypotension (IOH) prediction using Mean Arterial Pressure (MAP) is a critical research area with significant implications for patient outcomes during surgery. However, existing approaches predominantly employ static modeling paradigms that overlook the dynamic nature of physiological signal. In this paper, we introduce a novel Hybrid Multi-Factor (HMF) framework that reformulates IOH prediction as a blood pressure forecasting task. Our framework leverages a Transformer encoder, specifically designed to effectively capture the temporal evolution of MAP series through a patch-based input representation, which segments the input physiological series into informative patches for accurate analysis. To address the challenges of distribution shift in physiological series, our approach incorporates two key innovations: (1) Symmetric normalization and denormalization processes help mitigate distributional drift in statistical properties, thereby ensuring the model's robustness across varying conditions, and (2) Sequence decomposition, which disaggregates the input series into trend and seasonal components, allowing for a more precise modeling of inherent sequence dependencies. Extensive experiments conducted on two real-world datasets demonstrate the superior performance of our approach compared to competitive baselines, particularly in capturing the nuanced variations in input series that are crucial for accurate IOH prediction.

Introduction

Intraoperative mortality has decreased by a factor of 100 over the past century, making deaths during surgery a rare occurrence (Li et al. 2009; Monk et al. 2015). However, mortality within the first month following surgery remains a significant concern, with approximately 2% of patients undergoing inpatient noncardiac surgery dying within 30 days postoperatively (Spence et al. 2019)—amounting to more than 4 million deaths worldwide each year (Saugel and Sessler 2021). These postoperative deaths are most strongly linked to complications, which are often triggered by intraoperative events. Among these, intraoperative hypotension (IOH) is a common and serious complication (Kim et al. 2023), characterized by a significant drop in Mean Arterial Pressure (MAP) sustained over a period of time. IOH

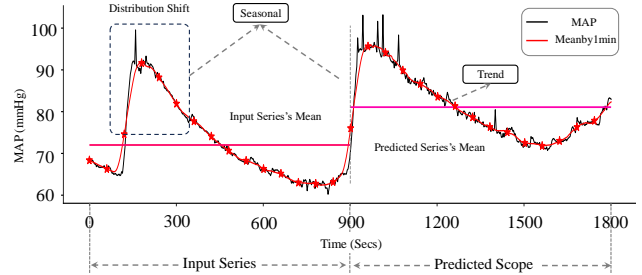


Figure 1: Illustration of MAP Series Characteristics: Distribution Shifts and Temporal Components in Intraoperative Hypotension Prediction.

is closely associated with adverse outcomes, including postoperative mortality, acute kidney injury, and myocardial injury (Hwang et al. 2023a; Fernandes et al. 2021).

Fortunately, it has been reported (Hatib et al. 2018a) that such events can be predicted using machine learning techniques applied to specific time intervals of MAP series. Meanwhile, clinical studies (Wijnberge et al. 2020) involving control group experiments have shown that early hypotension warnings and timely interventions can effectively reduce the severity of hypotension and reduce postoperative complications and mortality. In recent years, there has been notable progress in the study of IOH prediction. Through a systematic review of existing research, we found that the predominant modeling approaches involve predicting the risk of IOH events based on feature extraction (Lee et al. 2021b; Davies et al. 2020) combined with machine learning classifiers, such as logistic regression and random forests. While these methods are effective, they have two significant limitations: first, they primarily rely on static feature extraction (Lu et al. 2023a), which fails to capture the dynamic evolution of MAP series; second, their modeling approach lacks the flexibility to fully address the complexities of real-world clinical requirement scenarios. It is also widely recognized that the definition of IOH event is not universally standardized. For example, in clinical practice, using a fixed threshold may not accurately define IOH event, especially for hypertensive patients or the elderly, where more nuanced criteria are often necessary.

To address the limitations of current approaches, we explore IOH prediction from a novel perspective by reformu-

*corresponding author

lating it as a time series forecasting problem. Given that hypotensive events are defined by MAP series, this modeling approach offers greater flexibility, as the accuracy of future series forecasting directly influences the identification of risk events. However, as shown in Figure 1, several challenges arise when modeling MAP series forecasting: (1) *Non-stationary nature*: Sudden distribution shifts in blood pressure alter the statistical properties (e.g., mean and standard deviation) of the MAP series, complicating the maintenance of consistent predictive accuracy. (2) *Complex sequence structure*: The ABP signal comprises multiple components, such as trend and seasonal elements, which must be individually modeled for accurate forecasting. (3) *High sampling ratio*: The extended length of input series increases computational complexity in sequence modeling, complicating the representation learning process.

To address these challenges, we propose a Hybrid Multi-Factor (HMF) framework for dynamic IOH prediction. Our framework effectively models the non-stationary and complex nature of MAP series evolving during surgery. It introduces symmetric normalization and de-normalization techniques to counteract distributional drift in MAP series, ensuring robust performance across diverse patient conditions. Additionally, we leverage sequence decomposition to separately model the trend and seasonal components of the MAP series, enhancing the granularity of physiological insights. A patch-based Transformer encoder is employed to capture the dynamic evolution within the MAP series, enabling precise forecasting of hypotensive events. The effectiveness of our framework is validated through extensive experiments on two real-world datasets, demonstrating significant improvements over existing methods and underscoring its potential to enhance patient outcomes during surgery.

The main contributions of this work are as follows:

- We reformulate IOH prediction as an MAP series forecasting task and propose a Hybrid Multi-Factor (HMF) framework that integrates sequence decomposition with dynamic trend analysis.
- We identify two critical challenges that arise from formalizing intraoperative hypotension as MAP series forecasting, and we propose innovative solutions tailored to effectively address these challenges.
- We validate the effectiveness of HMF through comprehensive experiments on real-world datasets, achieving superior performance compared to compared baselines.

Preliminaries

To establish a solid foundation for our proposed approach, we first outline the essential concepts and definitions that underpin our methodology.

Dataset Description

Intraoperative hypotension (IOH) event poses significant risks to patient outcomes during surgery, necessitating reliable methods for early prediction and intervention. To address this, real-time monitoring and advanced modeling techniques are employed to capture the complex dynamics

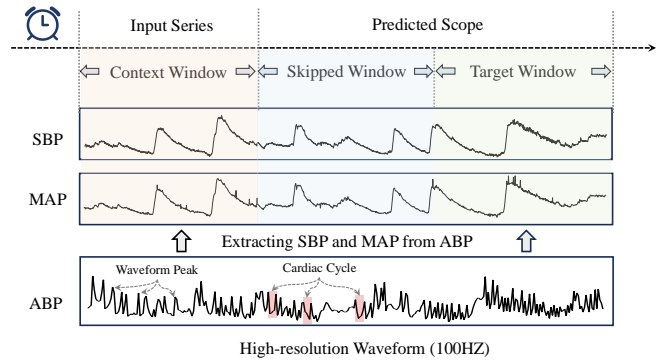


Figure 2: Feature Extraction and Temporal Window Setup for Blood Pressure Trend Prediction: Context, Skipped, and Target Windows.

of Arterial Blood Pressure (ABP) signal. By analyzing these series, we can identify patterns that precede hypotensive events, offering critical insights for timely clinical decision-making. The following sections introduce the fundamental concepts and methodologies that underpin our approach to IOH prediction, focusing on how we structure and utilize ABP signal for accurate forecasting.

Definition of Temporal Intervals. To effectively model the temporal dependencies inherent in ABP signal, we define several key concepts that structure the input series: *Context Window*, *Skipped Window*, and *Target Window*. The *Context Window* refers to the segment of the MAP and SBP series used as input to the prediction model. This window captures the historical dynamics of the series, providing the necessary context for accurate forecasting. The *Skipped Window* represents a temporal gap following the context window, with no predictions made during this period. This gap is introduced to prevent the model from overfitting to short-term fluctuations and to encourage the learning of longer-term dependencies. Finally, the *Target Window* is the segment of the series that the model is tasked with predicting. It represents the future time period of MAP. As illustrated in Figure 2, these windows are applied to segments of the ABP signal, with the context window providing input series, the skipped window allowing for temporal separation, and the target window representing the prediction objective.

Blood Pressure Feature Extraction. During surgery, advanced sensor is typically employed to continuously monitor a patient’s ABP signal in real-time, enabling precise oversight of blood pressure fluctuations. The core principle behind this approach is that specific patterns may emerge in the ABP signal before the patient is at risk of a hypotensive event. Previous studies have established a significant correlation between the variations in the blood pressure series within the context window and the subsequent onset of hypotension. It is important to note that ABP signal are typically sampled at high frequencies, such as 100 Hz, resulting in 100 samples per second. Despite this, ABP itself is not directly used to define hypotension. Instead, IOH event is commonly defined using the Mean Arterial Pressure (MAP) series, with hypotension typically characterized by MAP se-

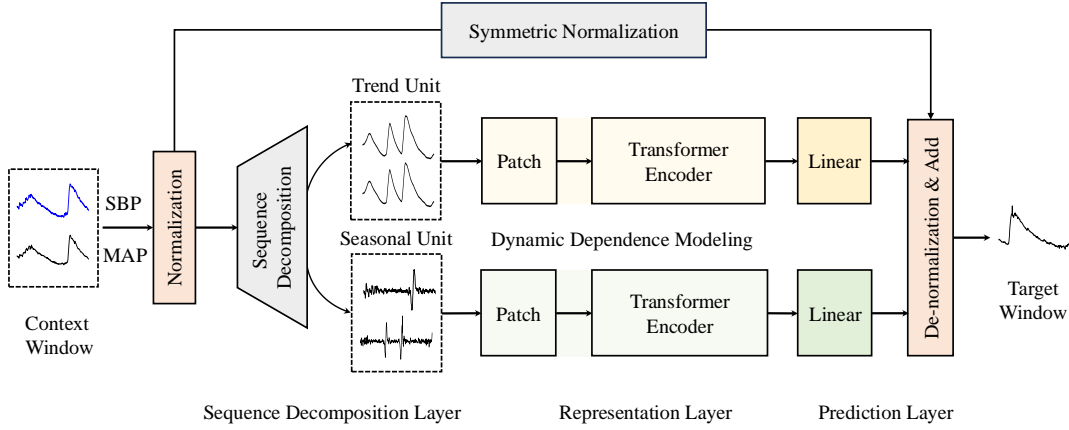


Figure 3: Proposed Hybrid Multi-Factor Model Architecture for Intraoperative Hypotension Prediction.

ries falling below a certain threshold for a sustained period, such as one minute. MAP is a series extracted from the ABP signal, specifically representing the average pressure within a single cardiac cycle. Additionally, Systolic Blood Pressure (SBP) is often incorporated as a feature in modeling blood pressure variations, due to the physiological relationship between SBP and MAP series. SBP series is derived from ABP signal by identifying the peak of each cardiac cycle. Together, these derived MAP and SBP series as the primary features for the forecasting task, enabling the model to focus on the clinically relevant aspects of blood pressure dynamics. Figure 2 also illustrates how to extract these features from the ABP signal and the defined temporal windows.

Problem Definition

In this study, we consider an input sequence $\mathbf{X} \in \mathbb{R}^{L \times 2}$ that comprises both the MAP and SBP series from a historical context window. Specifically, we redefine the task of IOH event prediction as a sequence forecasting problem. The objective is to predict the evolving trend of MAP over a future prediction window, thereby enabling early detection of potential hypotensive events during surgery. Formally, let $\mathbf{X} = \{\mathbf{X}_{\text{MAP}}, \mathbf{X}_{\text{SBP}}\}$, where $\mathbf{X}_{\text{MAP}} = \{x_{\text{MAP}}^1, x_{\text{MAP}}^2, \dots, x_{\text{MAP}}^T\}$ and $\mathbf{X}_{\text{SBP}} = \{x_{\text{SBP}}^1, x_{\text{SBP}}^2, \dots, x_{\text{SBP}}^T\}$ represent the MAP and SBP input sequences over a historical context window of length T . The goal is to predict the future MAP and SBP values $\hat{\mathbf{Y}} = \{\hat{\mathbf{Y}}_{\text{MAP}}, \hat{\mathbf{Y}}_{\text{SBP}}\}$, where $\hat{\mathbf{Y}}_{\text{MAP}} = \{\hat{y}_{\text{MAP}}^{T+1}, \hat{y}_{\text{MAP}}^{T+2}, \dots, \hat{y}_{\text{MAP}}^{T+\tau}\}$ and $\hat{\mathbf{Y}}_{\text{SBP}} = \{\hat{y}_{\text{SBP}}^{T+1}, \hat{y}_{\text{SBP}}^{T+2}, \dots, \hat{y}_{\text{SBP}}^{T+\tau}\}$ over the target window of length τ . The predictive model is designed to learn the temporal dynamics, capturing the intricate patterns and dependencies that influence MAP and SBP series. By forecasting the future MAP and SBP series, the model aims to assess whether the predicted MAP series fall below a critical threshold θ_{MAP} (Wesselink et al. 2018), thereby providing an early warning for potential IOH events.

The Proposed HMF

Hybrid Multi-Factor Framework Overview

The HMF model is an advanced multi-factor framework specifically designed for dynamic prediction of Intraoperative hypotension (IOH) event. By integrating Mean Arterial Pressure (MAP) and Systolic Blood Pressure (SBP) series, the model effectively captures the intricate nonlinear dynamics. The framework is structured into several key components: normalization, series decomposition, feature representation, and prediction. First, the model normalizes MAP and SBP series to reduce inter-patient variability, ensuring consistency across diverse patient profiles. The normalized series are then decomposed into trend and seasonal components, which enables the model to identify underlying patterns more effectively. The feature extraction process is powered by a Transformer encoder, which captures features with high effectiveness. These features are then seamlessly fused through a linear layer, allowing them for accurate forecasting. To address the challenge of rapid MAP series, the HMF model employs an autoregressive optimization strategy, which progressively generates future series based on the last segment within the context window, allowing the model to stay responsive to quick changes in MAP series.

Symmetric Normalization

Non-stationarity in MAP and SBP series, often caused by physiological factors during surgery, leads to sudden shifts in their statistical properties, such as mean and standard deviation (Kim et al. 2021). These abrupt changes complicate the maintenance of consistent predictive accuracy for IOH event. To address this, we introduce a symmetric normalization module to stabilize the MAP and SBP series, mitigating the impact of these shifts and ensuring more reliable predictions. Given a context window $X \in \mathbb{R}^{L \times 2}$, instance normalization is applied to produce the normalized sequence X' . The normalization is performed as follows:

$$X' = \frac{X - \mu_X}{\sigma_X},$$

Here, μ_X and σ_X represent the mean and standard deviation of the context window X . This step is vital for addressing the non-stationarity of the MAP and SBP series, allowing the model to focus on relative changes rather than absolute values. By normalizing the data, it mitigates the impact of distribution shifts, enabling the model to more effectively capture the underlying trends and patterns.

After the model processes the normalized data and predicts the future series, de-normalization is applied to restore the original scale of the predictions. The de-normalization is performed using the inverse operation:

$$\hat{Y} = \hat{Y}' \cdot \sigma_X + \mu_X,$$

Where, \hat{Y}' is the predicted series, and \hat{Y} is the de-normalized output. This normalization and de-normalization process ensures that the predictions are robust while maintaining the original data characteristics.

Sequence Decomposition

The Arterial Blood Pressure (ABP) signal exhibits a complex waveform structure, consisting of multiple components like trend and periodic elements, which need to be individually modeled for accurate forecasting. After applying instance normalization, which results in the normalized sequence X' , it becomes essential to decouple the physiological series into its trend and seasonal components. This decomposition allows for more precise modeling of each component, improving the overall forecasting accuracy. We follow the methodology of previous work (Wu et al. 2021; Wang et al. 2024; Cleveland et al. 1990) to achieve this decoupling, enabling the model to better capture the inherent patterns in the ABP signal, is computed using:

$$\text{Trend} = \text{AvgPool}(\text{Padding}(X')),$$

$$\text{Seasonal} = X' - \text{Trend},$$

Here, AvgPool smooths the sequence by downsampling through averaging within a specified window, while Padding ensures full coverage across the entire sequence.

Representation Layer

Patch embedding. To accurately model the nuanced dynamics of MAP and SBP series during surgery, we first apply a patch embedding technique following the decomposition layer. This approach offers several key advantages: it reduces sequence length, thereby decreasing computational complexity and making it more efficient to process long sequences. Additionally, by capturing local information through patch-based modeling, the impact of outliers and noise is minimized, leading to more robust predictions.

Specifically, the decomposed components of the series $W \in \mathbb{R}^{L \times 2}$ are transformed into a compact representation $W_{\text{patch}} \in \mathbb{R}^{\frac{L}{S} \times d_{\text{model}}}$ using three 1D convolutional layers, where S denotes the patch length. The patch embedding is:

$$W_{\text{patch}} = \text{Conv1D}_3(W),$$

Here, Conv1D₃ represents the application of three consecutive 1D convolutional layers to W . The embedding dimension d_{model} is optimized to capture complex features from the MAP and SBP series, which enhances the model's ability to discern intricate patterns critical for IOH prediction.

Moreover, to better capture the temporal structure, we introduce learnable positional encodings, computed as:

$$W_{\text{pos}} = W_{\text{patch}} + \text{PositionalEncoding}(W_{\text{patch}}),$$

These positional encodings allow the model to distinguish between different positions within the sequence, preserving the temporal dependencies crucial for accurately predicting future MAP series. This is particularly important in IOH prediction, where the timing and order of events play a vital role in ensuring accurate and reliable forecasts.

Sequence Dependence Modeling. To effectively model the temporal dynamics, particularly for accurate IOH prediction, it is crucial to capture both short-term and long-term dependencies within the data. The Transformer encoder is particularly well-suited for this task due to its ability to model long-range dependencies, which are essential for understanding the complex patterns in MAP and SBP series.

After obtaining the patch embeddings X_{pos} through the process of patch embedding and the addition of positional encodings, we utilize a Transformer encoder to capture sequence dependencies. This approach is advantageous because the Transformer's self-attention mechanism allows the model to dynamically weigh the importance of each patch in the sequence. By focusing on key patterns and fluctuations, the model can better predict future MAP series, which is critical for identifying potential IOH event.

Given the positional embeddings $X_{\text{pos}} \in \mathbb{R}^{\frac{L}{S} \times d_{\text{model}}}$, the Transformer encoder processes these embeddings through a series of self-attention and feedforward layers to capture the interdependencies between different patches. The sequence dependencies are computed as follows:

$$Z = \text{TransformerEncoder}(W_{\text{pos}}),$$

Here, $Z \in \mathbb{R}^{\frac{L}{S} \times d_{\text{model}}}$ represents the output of the Transformer encoder, which encodes the relationships between various segments of the MAP and SBP series. By leveraging the self-attention mechanism, the Transformer enables the model to focus on the most relevant information, effectively capturing the intricate temporal dependencies required for accurate and reliable IOH prediction.

This methodology ensures that subtle patterns within the MAP series, which may only be discernible when considering the entire sequence, are accurately identified. Consequently, the use of the Transformer encoder enhances the model's ability to predict IOH event with high precision, making it an ideal choice for this type of analysis.

Prediction Layer

To ensure that the temporal patterns identified by the Transformer encoder are accurately reflected in the MAP series predictions, we map the sequence representation Z to the

prediction using a linear layer. This efficiently translates the features captured by the Transformer into precise predictions while preserving the sequence dependencies crucial for MAP forecasting. The transformation from $Z \in \mathbb{R}^{\frac{L}{S} \times d_{\text{model}}}$ to $Y \in \mathbb{R}^{\frac{L}{S} \times \frac{2TS}{L}}$ is defined as:

$$Y = Z \cdot W + b,$$

where W and b represent the transformation matrix and bias vector, respectively. This linear transformation has been proven effective in sequence forecasting(Zeng et al. 2023; Ekambaram et al. 2023), it ensures that the sequence dependencies modeled by the encoder are directly translated into accurate future MAP series.

Optimization Strategies

To improve prediction accuracy, we integrate a patch-based autoregressive method into our model. This approach begins with the final patch of decomposed component W , denoted as $Y_0 = W \frac{L}{S}$, and sequentially generates subsequent patches using the autoregressive formula:

$$P(Y'_{i+1}) = \prod_{j=1}^i P(Y'_{j+1}|Y'_j),$$

where Y'_{i+1} represents the next patch in the sequence. The predicted sequence \hat{Y}' is:

$$\hat{Y}' = \{Y'_1, Y'_2, \dots, Y'_T\},$$

This method utilizes the context of preceding patches to enhance the model’s ability to capture temporal dependencies crucial for MAP forecasting. We optimize the model by minimizing the mean squared error (MSE) between the predicted sequence \hat{Y} and the actual target sequence Y :

$$\text{MSE} = \frac{1}{T} \sum_{t=1}^T (Y_t - \hat{Y}_t)^2,$$

This process ensures robust and accurate forecasts, making the model highly effective for IOH prediction.

Experiments

Experimental Setup

Dataset Description. We conduct experiments on two real-world datasets: **CH-OPBP** and **VitalDB**(Lee and Jung 2018) dataset. The **CH-OPBP**, a proprietary collection, initially contains 3,422 patient records with intraoperative blood pressure data recorded at a frequency of 100Hz. To standardize the data, it is resampled at 1-second and 3-second intervals, resulting in 1,083 records after discarding those shorter than 1 hour. Data acquisition for this dataset took place between February 27, 2023, and August 4, 2023. The **VitalDB** dataset initially comprises 6,388 records, which are resampled at 3-second intervals. Records with more than 20% missing data are excluded, resulting in a final dataset of 1,522 records. Both datasets are split into training, validation, and test sets in proportions of 80%,

10%, and 10%, respectively. Subsequently, these datasets are concatenated. Further details are available in Appendix A.

Implement Details. In our research, we utilize the forecasted Mean Arterial Pressure(MAP) series derived from the physiological series predictions of both MAP and Systolic Blood Pressure(SBP) series as the basis for classifying Intra-operative hypotension(IOH) event. Specifically, we employ a 15-minute context window as input, generating predicted scope over sequence lengths of 5, 10, and 15 minutes to effectively capture both short-term and long-term trends. The model is trained to minimize MSE between prediction and the ground-truth. We evaluate the model using both MSE and Mean Absolute Error (MAE), with particular emphasis on segments representing hypotensive data points. Although both MAP and SBP series are predicted during the time series forecasting phase, IOH event classification is based solely on the predicted MAP series in the target window. The skipped window is two minutes(Wijnberge et al. 2020). We outline the process of detecting IOH event through point-wise classification by comparing the predicted MAP series with the actual outcomes. The model’s performance is assessed using key metrics: accuracy, recall, and Area Under the Curve (AUC), with AUC being particularly vital for evaluating the model’s ability to distinguish between IOH event. Further details are provided in Appendix A.

Compared Baselines

As for traditional approaches, in our research, we employ ARIMA(Ariyo, Adewumi, and Ayo 2014) and Logistic Regression(Hosmer, Lemeshow, and Sturdivant 2000) as baseline models. ARIMA, a conventional time series forecasting technique, utilizes 0.5% of the test set data to ensure computational efficiency. Logistic Regression, often utilized for binary classification, is enhanced by integrating 1,566 features extracted using the tsfresh library¹. This model is evaluated through instance-based evaluation on 1% of the dataset. In terms of deep learning methods, We select LSTM (Graves and Graves 2012), Transformer (Vaswani et al. 2017), Informer (Zhou et al. 2021), and DLinear (Zeng et al. 2023) as our deep learning baselines. LSTM is effective at capturing long-term dependencies in sequences. The Transformer, with its self-attention mechanism, excels at handling long-range dependencies. Informer enhances the Transformer by incorporating a sparse attention mechanism, optimizing it for long sequence forecasting. DLinear is a linear model that efficiently captures trend and seasonality.

Experimental Results

Main Results Analysis. Table 1 provides a comprehensive evaluation of various predictive models for the critical task of dynamic IOH prediction, highlighting the superior performance of the HMF model.

The results demonstrate that the HMF model consistently outperforms baseline methods in both predictive accuracy and classification tasks across different datasets and sampling rates. Specifically, the HMF model achieves the lowest MSE and MAE values across all datasets, underscoring

¹<https://github.com/blue-yonder/tsfresh>

Table 1: Performance Comparison of Different Methods Using CH-OPBP and VitalDB .

Datasets	Sample(s)	Model	MSE	MAE	AUC	Accuracy (%)	Recall (%)
CH-OPBP	1	Arima	130.2702	8.8526	0.5963	77.32	24.00
		logistics	N/A	N/A	0.5054	76.08	35.10
		LSTM	118.1246	9.0985	0.5295	76.78	6.58
		Transformer	126.7972	9.3809	0.5919	75.63	22.43
		Informer	103.7028	8.0757	0.6452	72.26	35.38
		DLinear	125.6786	9.3232	0.5331	71.60	7.54
		HMF	93.2677	7.5823	0.7352	75.29	67.98
CH-OPBP	3	Arima	112.9281	8.1606	0.5928	75.70	25.65
		logistics	N/A	N/A	0.6774	75.71	54.49
		LSTM	124.4213	9.8814	0.5000	75.53	0.00
		Transformer	104.8545	8.3441	0.5970	74.44	23.12
		Informer	111.0393	8.3883	0.6278	79.81	30.37
		DLinear	123.8899	9.2951	0.5413	74.10	11.98
		HMF	86.4927	7.2828	0.7413	61.38	70.13
VitalDB	3	Arima	257.3701	13.1127	0.5250	59.31	8.53
		logistics	N/A	N/A	0.5595	62.60	33.47
		LSTM	188.7123	11.8613	0.5000	75.62	0.00
		Transformer	158.7031	10.6901	0.5040	73.51	0.93
		Informer	158.7873	10.8987	0.5003	75.01	0.05
		DLinear	175.1144	11.4968	0.5074	65.09	1.86
		HMF	165.7575	9.3845	0.6468	69.27	45.87

its exceptional capability to capture the intricate dynamics of blood pressure trend. This performance is particularly impressive given the non-stationary and complex nature of intraoperative blood pressure data, where traditional models often fail to maintain precision. Furthermore, HMF’s consistent performance improvements across varying sampling rates reflect its robustness in handling diverse temporal patterns under different data resolutions. In terms of the downstream IOH classification task, the HMF model excels by achieving the highest AUC and Recall values across all datasets and sampling rates, underscoring its effectiveness in detecting IOH events. For instance, on the CH-OPBP, the HMF model significantly outperforms other models, as evidenced by its superior AUC and Recall metrics, indicating a more reliable and sensitive detection of hypotensive events. This strong performance is maintained across both 1-second and 3-second sampling rates, demonstrating the model’s adaptability to different temporal granularities. Such adaptability is crucial in clinical settings where accurate IOH prediction can significantly impact patient outcomes. In contrast, while models like LSTM and Transformer offer competitive performance in some metrics, they often falter in scenarios involving long sequence dependencies and complex coupling effects—challenges that the HMF model effectively addresses through its specialized sequence dependence modeling. Informer and DLinear, despite their strengths in certain forecasting tasks, struggle with the complex temporal patterns in intraoperative data, particularly in recall performance. The HMF model’s ability to maintain high predictive accuracy performance across various conditions and data configurations underscores the significance of its novel design in effectively managing the complexities of intraoperative blood pressure trend.

Ablation Study. To further investigate the contribution of individual components within the HMF framework, we con-

ducted an ablation study on the CH-OPBP.

Table 2 clearly illustrates the crucial roles that instance normalization and sequence decomposition play in the effectiveness of the HMF model for predicting MAP series and detecting IOH events. The complete HMF model, which integrates both components, demonstrates superior performance across all metrics, achieving the lowest MSE and MAE on hypotensive data points, as well as the highest AUC and Recall, highlighting its exceptional accuracy. Removing instance normalization results in a significant increase in MSE and MAE on the hypotensive data points, along with a noticeable decline in AUC and Recall. This indicates that instance normalization is critical for addressing the non-stationary nature of intraoperative blood pressure data. Without normalization, the model struggles to manage the inherent variability in the data, leading to reduced precision and sensitivity, particularly in detecting IOH events. Similarly, the exclusion of sequence decomposition leads to a significant decline in performance, especially in terms of AUC and Recall. sequence decomposition is essential for disentangling the complex coupling between different temporal dynamics within blood pressure data. Without this decomposition, the model is unable to capture the underlying patterns and trends in the series, leading to inferior performance.

Transfer Study. In the medical domain, particularly for IOH prediction, it is crucial to assess the transferability of predictive models across different patients and demographic groups. Transfer learning is key to evaluating the robustness and generalizability of the HMF framework across diverse patient populations. To explore this, we applied the HMF model, initially trained on the CH-OPBP, to new patients and age groups. We then compared the model’s performance with and without transfer learning.

Table 3 presents the results of cross-patient transfer learning, where the HMF model trained on one patient was di-

Table 2: Ablation Study on CH-OPBP.

Dataset	Model	MSE	MAE	AUC	Accuracy (%)	Recall (%)
CH-OPBP	HMF	86.4927	7.2828	0.7413	75.53	70.13
	w/o instance normalization	106.9671	8.5005	0.5891	77.72	20.73
	w/o sequence decomposition	105.7231	8.4964	0.5750	78.10	17.50

rectly applied to another. The AUC results indicate that transfer learning not only maintains but in some cases enhances performance across different patients. This demonstrates the model’s ability to generalize shared patterns and trends across individuals, which is particularly valuable in the medical field where patient series can vary significantly. The success of transfer learning suggests that leveraging group-level data can improve individual prediction, reducing the need for extensive patient-specific series collection while still delivering accurate results. However, in certain cases where unique physiological factors are more pronounced, patient-specific training might still offer a slight advantage. Overall, transfer learning proves to be a powerful approach, enabling robust and reliable prediction across diverse patient populations in dynamic clinical settings.

Table 4 examines cross-feature transfer learning between age groups. In the elderly group, the non-transfer model achieves a higher AUC, suggesting that age-specific models may better capture the unique physiological complexities of older patients, who often present with comorbidities and age-related changes affecting blood pressure dynamics. In contrast, the younger group shows a slight AUC advantage with transfer learning, indicating that younger patients, with more homogeneous physiological responses, benefit from models trained on broader, age-inclusive data. These results highlight the importance of demographic-specific considerations in medical predictive models, where tailored approaches may be necessary for certain populations, while transfer learning can effectively generalize across others.

Table 3: Comparison of Cross-Patient Performance with and without Transfer Learning.

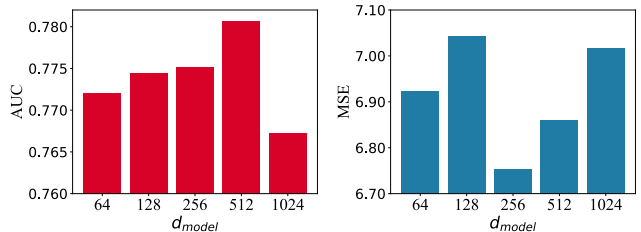
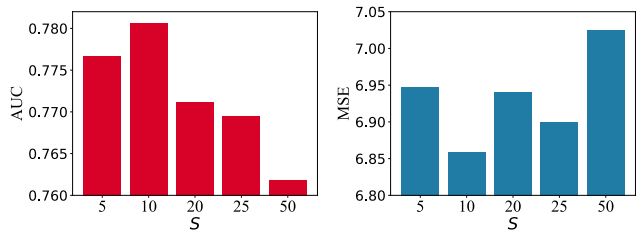
	Patient ID	MSE	MAE	AUC
Transfer	1	37.3299	5.6241	0.5375
	2	39.9698	6.2213	0.6100
Non-Transfer	1	18.6823	3.8187	0.2375
	2	47.6620	6.8317	0.5600

Table 4: Comparison of Cross-Feature Performance with and without Transfer Learning.

	Feature	MSE	MAE	AUC
Transfer	Elderly	118.9462	9.1424	0.6089
	Young	38.0568	5.0047	0.8040
Non-Transfer	Elderly	66.5058	6.5874	0.7850
	Young	44.1721	5.2447	0.8540

Parameter Sensitivity Analysis Experiment. We conducted a parameter sensitivity analysis on the CH-OPBP to optimize key model parameters, specifically d_{model} and patch length S , which are critical for the Patch Encoder’s ability to capture temporal dependencies. The analysis began by varying d_{model} while maintaining a fixed context window of 300 and a predicted scope length of 100. The optimal d_{model}

value, which maximizes model performance, is presented in Figure 4. Subsequently, we assessed the impact of varying S values while keeping d_{model} constant. This step was crucial for identifying the most effective S value, as it significantly influences the model’s performance. The results of this analysis are shown in Figure 5. Based on these analyses, we selected the parameter values that yielded the highest AUC scores, thereby ensuring optimal model performance. The sensitivity of the model’s performance to these parameters highlights the critical role of the Patch Encoder in accurately modeling blood pressure patterns.

Figure 4: Analysis of MSE and AUC performance for IOH segments across varying $d_{\text{model}} \in \{64, 128, 256, 512, 1024\}$.Figure 5: Analysis of MSE and AUC performance for IOH segments across varying $S \in \{5, 10, 20, 25, 50\}$.

Conclusion

In this paper, we introduced a novel approach to IOH prediction by framing the problem as a time series forecasting task. We highlighted the challenges associated with this new modeling paradigm and proposed targeted strategies. Specifically, we employed symmetric normalization techniques to mitigate the non-stationary nature of Mean Arterial Pressure (MAP) and Systolic Blood Pressure (SBP) series, and leveraged sequence decomposition to handle the complex series structure. Additionally, our patch-based Transformer model efficiently learned the representations of MAP and SBP series, enabling accurate forecasting. Our extensive experiments on real-world datasets demonstrated the effectiveness of the proposed HMF framework. We hope that this work provides a fresh perspective on the early warning of IOH events and inspires future research in this critical area.

References

- Ariyo, A. A.; Adewumi, A. O.; and Ayo, C. K. 2014. Stock Price Prediction Using the ARIMA Model. In *2014 UKSim-AMSS 16th International Conference on Computer Modelling and Simulation*, 106–112.
- Chen, M.; Peng, H.; Fu, J.; and Ling, H. 2021. Autoformer: Searching transformers for visual recognition. In *Proceedings of the IEEE/CVF international conference on computer vision*, 12270–12280.
- Cheng, M.; Liu, Q.; Liu, Z.; Li, Z.; Luo, Y.; and Chen, E. 2023a. Formertime: Hierarchical multi-scale representations for multivariate time series classification. In *Proceedings of the ACM Web Conference 2023*, 1437–1445.
- Cheng, M.; Liu, Q.; Liu, Z.; Zhang, H.; Zhang, R.; and Chen, E. 2023b. Timemae: Self-supervised representations of time series with decoupled masked autoencoders. *arXiv preprint arXiv:2303.00320*.
- Cheng, M.; Yang, J.; Pan, T.; Liu, Q.; and Li, Z. 2024. ConvtimeNet: A deep hierarchical fully convolutional model for multivariate time series analysis. *arXiv preprint arXiv:2403.01493*.
- Cherifa, M.; Blet, A.; Chambaz, A.; Gayat, E.; Resche-Rigon, M.; and Pirracchio, R. 2020. Prediction of an acute hypotensive episode during an ICU hospitalization with a super learner machine-learning algorithm. *Anesthesia & Analgesia*, 130(5): 1157–1166.
- Cleveland, R. B.; Cleveland, W. S.; McRae, J. E.; Terpenning, I.; et al. 1990. STL: A seasonal-trend decomposition. *J. off. Stat.*, 6(1): 3–73.
- Davies, S. J.; Vistisen, S. T.; Jian, Z.; Hatib, F.; and Scheeren, T. W. 2020. Ability of an arterial waveform analysis-derived hypotension prediction index to predict future hypotensive events in surgical patients. *Anesthesia & Analgesia*, 130(2): 352–359.
- Dey, R.; and Salem, F. M. 2017. Gate-variants of gated recurrent unit (GRU) neural networks. In *2017 IEEE 60th international midwest symposium on circuits and systems (MWSCAS)*, 1597–1600. IEEE.
- Ekambaram, V.; Jati, A.; Nguyen, N.; Sinthong, P.; and Kalagnanam, J. 2023. Tsmixer: Lightweight mlp-mixer model for multivariate time series forecasting. In *Proceedings of the 29th ACM SIGKDD Conference on Knowledge Discovery and Data Mining*, 459–469.
- Fernandes, M. P. B.; de la Hoz, M. A.; Rangasamy, V.; and Subramaniam, B. 2021. Machine learning models with pre-operative risk factors and intraoperative hypotension parameters predict mortality after cardiac surgery. *Journal of Cardiothoracic and Vascular Anesthesia*, 35(3): 857–865.
- Graves, A.; and Graves, A. 2012. Long short-term memory. *Supervised sequence labelling with recurrent neural networks*, 37–45.
- Hatib, F.; Jian, Z.; Buddi, S.; Lee, C.; Settels, J.; Sibert, K.; Rinehart, J.; and Cannesson, M. 2018a. Machine-learning algorithm to predict hypotension based on high-fidelity arterial pressure waveform analysis. *Anesthesiology*, 129(4): 663–674.
- Hatib, F.; Jian, Z.; Buddi, S.; Lee, C.; Settels, J.; Sibert, K.; Rinehart, J.; and Cannesson, M. 2018b. Machine-learning algorithm to predict hypotension based on high-fidelity arterial pressure waveform analysis. *Anesthesiology*, 129(4): 663–674.
- He, W.; Cheng, M.; Liu, Q.; and Li, Z. 2023. Shapewordnet: An interpretable shapenet neural network for physiological signal classification. In *International Conference on Database Systems for Advanced Applications*, 353–369. Springer.
- Hosmer, D. W.; Lemeshow, S.; and Sturdivant, R. X. 2000. *Applied logistic regression*. Wiley New York.
- Hwang, E.; Park, Y.-S.; Kim, J.-Y.; Park, S.-H.; Kim, J.; and Kim, S.-H. 2023a. Intraoperative hypotension prediction based on features automatically generated within an interpretable deep learning model. *IEEE Transactions on Neural Networks and Learning Systems*.
- Hwang, E.; Park, Y.-S.; Kim, J.-Y.; Park, S.-H.; Kim, J.; and Kim, S.-H. 2023b. Intraoperative hypotension prediction based on features automatically generated within an interpretable deep learning model. *IEEE Transactions on Neural Networks and Learning Systems*.
- Jeong, Y.-S.; Kang, A. R.; Jung, W.; Lee, S. J.; Lee, S.; Lee, M.; Chung, Y. H.; Koo, B. S.; and Kim, S. H. 2019. Prediction of blood pressure after induction of anesthesia using deep learning: A feasibility study. *Applied Sciences*, 9(23): 5135.
- Kang, A. R.; Lee, J.; Jung, W.; Lee, M.; Park, S. Y.; Woo, J.; and Kim, S. H. 2020. Development of a prediction model for hypotension after induction of anesthesia using machine learning. *PloS one*, 15(4): e0231172.
- Kendale, S.; Kulkarni, P.; Rosenberg, A. D.; and Wang, J. 2018. Supervised machine-learning predictive analytics for prediction of postinduction hypotension. *Anesthesiology*, 129(4): 675–688.
- Kim, J.; Kim, S.-H.; Hwang, E.; Park, Y.-S.; Kim, J.-Y.; and Park, S.-H. 2023. Intraoperative Hypotension Prediction Based on Features Automatically Generated Within an Interpretable Deep Learning Model. *Authorea Preprints*.
- Kim, T.; Kim, J.; Tae, Y.; Park, C.; Choi, J.-H.; and Choo, J. 2021. Reversible instance normalization for accurate time-series forecasting against distribution shift. In *International Conference on Learning Representations*.
- Lee, H.; Yun, D.; Yoo, J.; Yoo, K.; Kim, Y. C.; Kim, D. K.; Oh, K.-H.; Joo, K. W.; Kim, Y. S.; Kwak, N.; et al. 2021a. Deep learning model for real-time prediction of intradialytic hypotension. *Clinical Journal of the American Society of Nephrology*, 16(3): 396–406.
- Lee, H.-C.; and Jung, C.-W. 2018. Vital Recorder—a free research tool for automatic recording of high-resolution time-synchronised physiological data from multiple anaesthesia devices. *Scientific reports*, 8(1): 1527.
- Lee, S.; Lee, H.-C.; Chu, Y. S.; Song, S. W.; Ahn, G. J.; Lee, H.; Yang, S.; and Koh, S. B. 2021b. Deep learning models for the prediction of intraoperative hypotension. *British journal of anaesthesia*, 126(4): 808–817.

- Lee, S.; Lee, H.-C.; Chu, Y. S.; Song, S. W.; Ahn, G. J.; Lee, H.; Yang, S.; and Koh, S. B. 2021c. Deep learning models for the prediction of intraoperative hypotension. *British journal of anaesthesia*, 126(4): 808–817.
- Lee, S.; Lee, M.; Kim, S.-H.; and Woo, J. 2022. Intraoperative hypotension prediction model based on systematic feature engineering and machine learning. *Sensors*, 22(9): 3108.
- Li, G.; Warner, M.; Lang, B. H.; Huang, L.; and Sun, L. S. 2009. Epidemiology of anesthesia-related mortality in the United States, 1999–2005. In *The Journal of the American Society of Anesthesiologists*, volume 110, 759–765. The American Society of Anesthesiologists.
- Liu, Z.; Yang, J.; Cheng, M.; Luo, Y.; and Li, Z. 2024. Generative pretrained hierarchical transformer for time series forecasting. In *Proceedings of the 30th ACM SIGKDD Conference on Knowledge Discovery and Data Mining*, 2003–2013.
- Lu, F.; Li, W.; Zhou, Z.; Song, C.; Sun, Y.; Zhang, Y.; Ren, Y.; Liao, X.; Jin, H.; Luo, A.; et al. 2023a. A composite multi-attention framework for intraoperative hypotension early warning. In *Proceedings of the AAAI Conference on Artificial Intelligence*, volume 37, 14374–14381.
- Lu, F.; Li, W.; Zhou, Z.; Song, C.; Sun, Y.; Zhang, Y.; Ren, Y.; Liao, X.; Jin, H.; Luo, A.; et al. 2023b. A composite multi-attention framework for intraoperative hypotension early warning. In *Proceedings of the AAAI Conference on Artificial Intelligence*, volume 37, 14374–14381.
- Monk, T. G.; Bronsert, M. R.; Henderson, W. G.; Mangione, M. P.; Sum-Ping, S. J.; Bentt, D. R.; Nguyen, J. D.; Richman, J. S.; Meguid, R. A.; and Hammermeister, K. E. 2015. Association between intraoperative hypotension and hypertension and 30-day postoperative mortality in noncardiac surgery. *Anesthesiology*, 123(2): 307–319.
- Ritter, J.; Chen, X.; Bai, L.; and Huang, J. 2023. Predicting Hypotension by Learning from Multivariate Mixed Responses. In *Proceedings of the International MultiConference of Engineers and Computer Scientists 2023*.
- Saugel, B.; and Sessler, D. I. 2021. Perioperative blood pressure management. *Anesthesiology*, 134(2): 250–261.
- Spence, J.; LeManach, Y.; Chan, M. T.; Wang, C.; Sigamani, A.; Xavier, D.; Pearse, R.; Alonso-Coello, P.; Garutti, I.; Srinathan, S. K.; et al. 2019. Association between complications and death within 30 days after noncardiac surgery. *Cmaj*, 191(30): E830–E837.
- Tang, Y.; Brown, S.; Sorensen, J.; and Harley, J. B. 2019. Reduced rank least squares for real-time short term estimation of mean arterial blood pressure in septic patients receiving norepinephrine. *IEEE Journal of Translational Engineering in Health and Medicine*, 7: 1–9.
- Vaswani, A.; Shazeer, N.; Parmar, N.; Uszkoreit, J.; Jones, L.; Gomez, A. N.; Kaiser, Ł.; and Polosukhin, I. 2017. Attention is All You Need. In *Advances in Neural Information Processing Systems*, 5998–6008.
- Wang, S.; Wu, H.; Shi, X.; Hu, T.; Luo, H.; Ma, L.; Zhang, J. Y.; and Zhou, J. 2024. Timemixer: Decomposable multiscale mixing for time series forecasting. *arXiv preprint arXiv:2405.14616*.
- Wesselink, E.; Kappen, T.; Torn, H.; Slooter, A.; and Van Klei, W. 2018. Intraoperative hypotension and the risk of postoperative adverse outcomes: a systematic review. *British journal of anaesthesia*, 121(4): 706–721.
- Wijnberge, M.; Geerts, B. F.; Hol, L.; Lemmers, N.; Mulder, M. P.; Berge, P.; Schenk, J.; Terwindt, L. E.; Hollmann, M. W.; Vlaar, A. P.; et al. 2020. Effect of a machine learning–derived early warning system for intraoperative hypotension vs standard care on depth and duration of intraoperative hypotension during elective noncardiac surgery: the HYPE randomized clinical trial. *Jama*, 323(11): 1052–1060.
- Wu, H.; Xu, J.; Wang, J.; and Long, M. 2021. Autoformer: Decomposition Transformers with Auto-Correlation for Long-Term Series Forecasting. In Ranzato, M.; Beygelzimer, A.; Dauphin, Y.; Liang, P.; and Vaughan, J. W., eds., *Advances in Neural Information Processing Systems*, volume 34, 22419–22430. Curran Associates, Inc.
- Zeng, A.; Chen, M.; Zhang, L.; and Xu, Q. 2023. Are Transformers Effective for Time Series Forecasting? In *Proceedings of the AAAI Conference on Artificial Intelligence*, volume 37, 11121–11128.
- Zhou, H.; Zhang, S.; Peng, J.; Zhang, S.; Li, J.; Xiong, H.; and Zhang, W. 2021. Informer: Beyond Efficient Transformer for Long Sequence Time-Series Forecasting. In *Proceedings of the AAAI Conference on Artificial Intelligence*, volume 35, 11106–11115.
- Zhou, T.; Ma, Z.; Wen, Q.; Wang, X.; Sun, L.; and Jin, R. 2022. Fedformer: Frequency enhanced decomposed transformer for long-term series forecasting. In *International conference on machine learning*, 27268–27286. PMLR.

Appendices

Appendix A Related Work

Intraoperative Hypotension Forecasting

Numerous studies have developed models to predict intraoperative hypotension (IOH) using real-time biosignal and clinical data analysis. Early work focused on high-fidelity arterial pressure waveforms, leading to the development of a hypotension prediction index (HPI) that predicts IOH events up to 15 minutes in advance (Hatib et al. 2018b). Later research integrated multiple biosignals, like electrocardiography and photoplethysmography, to enhance prediction accuracy (Lee et al. 2021c). Feature engineering using statistical and frequency analyses of invasive blood pressure (IBP) data also demonstrated significant accuracy in IOH prediction models (Lee et al. 2022).

As the field advanced, supervised ensemble learning algorithms like Super Learner were employed to predict acute hypotensive episodes (AHE) during surgery, combining physiological signals and dynamic factors for strong predictive performance (Cherifa et al. 2020). Random forest models effectively predicted post-induction hypotension (PIH) during anesthesia induction (Kang et al. 2020), while

gradient boosting machines (GBM) highlighted the clinical potential by analyzing preoperative and intraoperative factors (Kendale et al. 2018).

Deep learning further advanced IOH prediction with bidirectional recurrent neural networks (RNNs) predicting blood pressure changes post-anesthesia induction with high accuracy (Jeong et al. 2019). Reduced-rank least squares models using ICU data, including heart rate and norepinephrine infusion rates, have shown promise in real-time mean arterial pressure (MAP) prediction (Tang et al. 2019).

Recent work introduced the Interpretable Neural Network (INN) approach, utilizing preoperative and intraoperative data to predict perioperative hypotension with high accuracy and interpretability, facilitating clinical adoption (Ritter et al. 2023). Additionally, the Composite Multi-Attention (CMA) framework integrated vital signs and demographics to predict customizable IOH events with high accuracy across large datasets (Lu et al. 2023b). Interpretable deep learning models predicting IOH 10 minutes in advance using brief arterial blood pressure recordings have generated clinically relevant predictors (Hwang et al. 2023b). These advancements provide a strong foundation for continued exploration in IOH prediction.

Time Series and Sequence Forecasting

Time series forecasting (Cheng et al. 2024) is crucial in domains such as finance, healthcare, and energy management. In physiological signal prediction (He et al. 2023), such as arterial blood pressure (ABP), traditional models like ARIMA (Ariyo, Adewumi, and Ayo 2014) and exponential smoothing are commonly used but often struggle with complex, high-dimensional data. Deep learning models, particularly RNN variants like LSTMs (Graves and Graves 2012) and GRUs (Dey and Salem 2017), are favored for their ability to capture long-term dependencies.

Recent advances in long-sequence time series forecasting (LSTF) focus on Transformer-based models. Informer (Zhou et al. 2021) reduces computational complexity using a ProbSparse self-attention mechanism, while Autoformer (Chen et al. 2021) introduces decomposition and auto-correlation mechanisms for long-term trend forecasting. FEDformer (Zhou et al. 2022) integrates seasonal-trend decomposition and frequency domain analysis to model global trends and fine-grained structures. TimeMAE (Cheng et al. 2023b) further improves time series classification by utilizing bidirectional encoding, masking strategies, and a decoupled autoencoder to enhance representation learning.

Despite the success of Transformers, challenges such as high computational costs and large data requirements remain. Models like FormerTime (Cheng et al. 2023a) address these issues by combining transformers and convolutional networks in a hierarchical framework, improving scalability and efficiency for multivariate time series classification. Simpler approaches, like DLinear (Zeng et al. 2023), demonstrate that linear models can outperform more complex ones by preserving temporal information, while TSMixer (Ekambaram et al. 2023) improves interaction modeling with a lightweight MLP-based architecture.

GPHT (Liu et al. 2024) introduces a generative pretrained hierarchical transformer for forecasting, leveraging mixed datasets and auto-regressive modeling to enhance transferability across different datasets and forecasting horizons. These advancements, particularly in arterial blood pressure (MAP) and intraoperative hypotension (IOH) prediction, highlight promising directions for combining lightweight and Transformer-based models to improve prediction accuracy and real-time clinical applications.

Appendix B Implementation Details

We summarized details of datasets, evaluation details, experiments details and visualizations in this section.

Datasets details

Data pre-processing. In this study, we implemented rigorous data cleaning procedures to ensure the high quality and accuracy of parameters extracted from Arterial Blood Pressure (ABP) signals. Initially, we screened the segments of the ABP signals to ensure they fell within a reasonable blood pressure range, thereby eliminating outliers and reducing noise interference. From these, we selected the longest continuous segments within the physiological range to ensure data continuity and reliability.

Subsequently, we conducted frequency analysis on the selected segments to further validate the stability and accuracy of the signals, removing portions that might be influenced by interference or abnormal heartbeats. This process ensured the precision of the data. In the processed signals, we extracted Systolic Blood Pressure (SBP) and Diastolic Blood Pressure (DBP) by identifying the maxima and minima within each cardiac cycle—defining the highest point as SBP and the lowest point as DBP. The Mean Arterial Pressure (MAP) was then calculated using the formula: $MAP = \frac{1}{3} \times SBP + \frac{2}{3} \times DBP$ (Lee et al. 2021a), which is based on the physiological model of arterial blood pressure.

Ground Truth Labeling. In this study, ground truth labels for intraoperative hypotension (IOH) events were generated using the actual MAP values recorded during the intraoperative period. The labeling process was designed to identify segments of the MAP series, defined as a MAP value less than or equal to θ_{MAP} mmHg, sustained for a minimum duration of t minutes. For our analysis, we set t to 1 minute. θ_{MAP} is typically set to 65 mmHg (Wesselink et al. 2018), a threshold widely used in clinical practice to identify hypotensive events. The algorithm iterates the actual MAP series, examining each segment of length t . For each segment, the maximum MAP value within that segment is determined. If this maximum value is less than or equal to θ_{MAP} , the corresponding segment is labeled as an IOH event. This labeling process ensures that only clinically relevant hypotensive events are captured, providing a robust ground truth for model evaluation. The algorithm used for generating the ground truth labels is detailed in Algorithm 1.

More details of dataset. The CH-OPBP initially contained 3,422 patient records with intraoperative blood pressure data recorded at 100Hz. To standardize the dataset, we

Algorithm 1: Ground Truth Labeling

Input: MAP_{actual} : actual sequence of MAP values, t : the minimum duration for an IOH event, T_{seq} : length of the MAP series for each patient.

Output: L_{actual} : the sequence of actual labels.

```
1: Let  $L_{\text{actual}}[:] = 0$ 
2: for  $i$  in range( $0, T_{\text{seq}} - t + 1$ ) do
3:    $MAP_{\text{max}} = \max(MAP_{\text{actual}}[i : i + t])$ 
4:   if  $MAP_{\text{max}} \leq \theta_{\text{MAP}}$  then
5:      $L_{\text{actual}}[i : i + t] = 1$ 
6:   end if
7: end for
8: return  $L_{\text{actual}}$ 
```

resampled the data at 1-second and 3-second intervals. After excluding records shorter than 1 hour, the final dataset comprised 1,083 records. Data collection occurred from February 27, 2023, to August 4, 2023.

This **CH-OPBP** has undergone rigorous anonymization processes to ensure that no personally identifiable information is included. Consequently, in accordance with current ethical guidelines, the use of this dataset is exempt from requiring formal ethical approval. Moreover, the research strictly adheres to all relevant legal and regulatory frameworks, and confidentiality agreements have been signed to ensure the security and privacy of the data. Data access is restricted to authorized personnel only, and all data use is confined to research purposes.

The **VitalDB** originally included 6388 patient records. We applied a 3-second sampling rate and excluded records with more than 20% missing data, resulting in a final dataset of 1522 records.

For both datasets, patient records were divided into training, validation, and test sets using an 80%, 10%, and 10% split, respectively. After splitting, data samples from each group were concatenated to form the final training, validation, and test datasets. This approach ensured that each set accurately reflected the overall data distribution, thereby supporting robust model evaluation.

A context window of 15 minutes was utilized to capture relevant features and context from the data. The CH-OPBP was sampled at granularities of 1 second and 3 seconds, while the VitalDB dataset was sampled at a granularity of 3 seconds. Based on these sampling rates, predictions were made for multiple sequence lengths—specifically 5, 10, and 15 minutes. This multi-length prediction strategy enabled a comprehensive analysis of both short-term and long-term trends within the prediction horizon.

When segmenting instances for the dataset, the prediction scope was divided using varying step sizes depending on the presence of hypotension. For instances where hypotension occurred within the prediction scope, a step size of 1 was used, allowing for finer granularity and more precise modeling of these critical events. Conversely, in the absence of hypotension, a step size of 10 was employed, optimizing processing efficiency while still capturing the necessary infor-

mation. Detailed information on the CH-OPBP and VitalDB datasets, including sampling rates and other relevant characteristics, is summarized in Table 5.

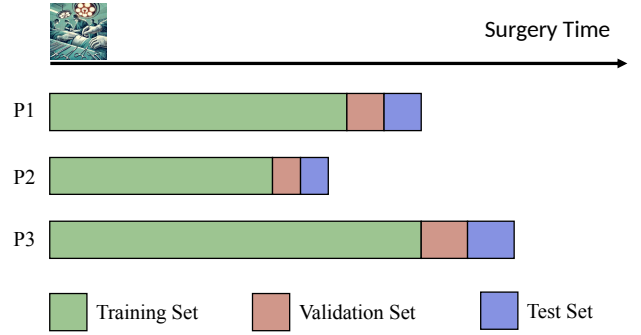


Figure 6: Patient Data Splitting Strategy.

Evaluation details

In our experiments, we first modeled time series prediction of mean arterial pressure (MAP), using this predicted MAP as a critical input for subsequent classification of intraoperative hypotension (IOH) events. The model, HMF, was trained to minimize mean squared error (MSE), measuring discrepancy between the predicted MAP values and ground truth. A lower MSE indicates a more accurate prediction. For detection of IOH events, we specifically focused on segments where the actual MAP label, L_{actual} , is 1, and computed both MSE and mean absolute error (MAE) for these segments to assess the model's performance.

Building on the predicted MAP values, Algorithm 2 outlines the process for evaluating IOH events by comparing actual and predicted scenarios. We assess the model's classification performance using several metrics, including accuracy, recall, and the area under the curve (AUC). Among these, the AUC is particularly crucial as it provides an overall measure of the model's ability to distinguish between IOH and non-IOH events. Our evaluation approach is based on a point-wise assessment method, which involves evaluating each individual data point for its classification accuracy. This method ensures a granular and precise evaluation of the model's performance. Additionally, in this study, we set a skipped window of 2 minutes, meaning that the evaluation focuses on the content of the target window, excluding data points within the skipped interval. We evaluated the performance of HMF using several key metrics: accuracy, recall, and AUC. Accuracy, defined as

$$\text{Accuracy} = \frac{TP + TN}{TP + TN + FP + FN},$$

represents the proportion of correctly classified instances among all instances, where TP (True Positive) denotes the number of correctly identified positive cases, TN (True Negative) indicates the correctly identified negative cases, FP (False Positive) represents the negative cases incorrectly identified as positive, and FN (False Negative) denotes the positive cases incorrectly identified as negative.

Table 5: Dataset Details.

Dataset	Patient num	Sampling Rate(s)	predicted scope	Training Set	Validation Set	Test Set
CH-OPBP	1083	1	300	442858	54406	58019
			600	489273	58810	66071
			900	519339	61776	71130
		3	100	148274	18243	19401
			200	164049	19719	22124
			300	174311	20764	23848
VitalDB	1522	3	100	466402	61158	58042
			200	589414	78037	74094
			300	689650	91902	87685

Algorithm 2: IOH Events Detection

Input: O_{pred} : predicted sequence of MAP values, t : minimum duration of IOH, T_{instance} : length of the target window, L_{actual} : actual labels sequence.

Output: J_{actual} : boolean indicating the presence of an IOH event in the actual instance, $J_{\text{prediction}}$: boolean indicating the presence of an IOH event in the predicted instance.

```

1:  $J_{\text{actual}} = 0$ 
2:  $J_{\text{prediction}} = 0$ 
3: for  $i$  in range( $0, T_{\text{instance}} - t + 1$ ) do
4:    $\text{sum}_{\text{actual}} = \text{sum}(L_{\text{actual}}[i : i + t])$ 
5:   if  $\text{sum}_{\text{actual}} > 0$  then
6:      $J_{\text{actual}} = 1$ 
7:   end if
8:    $\text{sum}_{\text{prediction}} = \sum_{j=0}^{t-1} (O_{\text{pred}}[i + j] \leq 65)$ 
9:   if  $\text{sum}_{\text{prediction}} > 0.8 * t$  then
10:     $J_{\text{prediction}} = 1$ 
11:  end if
12: end for
13: return  $J_{\text{actual}}, J_{\text{prediction}}$ 

```

Recall, expressed as

$$\text{Recall} = \frac{TP}{TP + FN},$$

indicates the proportion of actual positive cases that were correctly identified by the model.

Lastly, the AUC of the Receiver Operating Characteristic (ROC) curve provides a comprehensive measure of the model’s ability to discriminate between positive and negative cases. A higher AUC value indicates better overall performance, capturing both the model’s recall and specificity.

Experiment details

This study presents a model architecture specifically tailored to address the challenges of predicting intraoperative hypotension (IOH) events, where the non-stationary and complex nature of blood pressure trends poses significant difficulties for traditional models. The model leverages self-attention mechanisms to effectively capture long-range dependencies within the time series data, while multi-head attention facilitates a nuanced understanding of interactions

across different time steps. To mitigate the risk of overfitting—a critical concern given the variability and noise in intraoperative data—dropout was applied in both the self-attention layers and the feed-forward network.

The Adam optimizer was strategically chosen for its ability to maintain stable convergence across diverse parameter spaces, enhancing the model’s robustness. This approach ensured the model could reliably predict IOH events across a wide range of patient profiles and surgical scenarios, demonstrating its practical utility in clinical settings.

To ensure the fairness and comparability of results across different models and datasets, hyperparameters were systematically selected, and final results were averaged over multiple runs to reduce the impact of outliers and minimize potential overfitting in any single run. The experiments were executed on two distinct machines to maximize computational efficiency: an RTX 4090 GPU with 90GB of memory provided the substantial computational power required for deep learning tasks, while an AMD EPYC 7742 CPU with 192GB of memory was ideal for handling extensive data processing and parallel computations.

These carefully selected resources and methodologies ensured that the experiments were conducted in a robust and replicable manner, thereby enhancing confidence in the generalizability and reliability of the results.

Appendix C Baseline Details

To enhance the evaluation of HMF’s performance in early identification of IOH events, we employed a combination of traditional and deep learning-based prediction algorithms as benchmarks in our experiments.

Traditional Methods We employed two traditional methods as baselines:

- **ARIMA(Ariyo, Adewumi, and Ayo 2014)**: ARIMA was employed as one of the traditional baseline methods. Due to efficiency concerns, the ARIMA model was trained on only 0.5% of the test set data, ensuring that the computational load remained manageable while still providing a meaningful comparison against other models.
- **Logistic Regression(Hosmer, Lemeshow, and Sturdivant 2000)**: Logistic regression, a widely used statistical method for binary classification, was utilized as another baseline model. To enhance its performance, fea-

ture extraction was conducted using the tsfresh library², which automatically extracted 1,566 features from the time series data. This approach significantly improved the model’s ability to classify IOH events accurately.

Deep Learning Methods We included several deep learning-based methods in our benchmarks, each recognized for its ability to capture complex patterns in time series data:

- **LSTM(Graves and Graves 2012)**: The Long Short-Term Memory (LSTM) model was included in our benchmarks due to its strong ability to capture temporal dependencies in time series data. LSTM is particularly effective in handling sequences with long-term dependencies, making it a valuable baseline for comparison.
- **Transformer(Vaswani et al. 2017)**: The Transformer model, known for its self-attention mechanism, was employed as a baseline. This mechanism allows the model to weigh the importance of different time steps, enabling it to capture complex patterns and long-range dependencies, making it a robust choice for time series analysis.
- **Informer(Zhou et al. 2021)**: The Informer model, a variant of the Transformer, introduces sparse self-attention mechanisms to reduce computational complexity while maintaining the ability to capture critical dependencies in time series data. This efficiency makes Informer a powerful baseline for our benchmarks.
- **DLinear(Zeng et al. 2023)**: The DLinear model was also included as a baseline. DLinear is a linear model specifically designed for time series forecasting. Despite its simplicity, DLinear effectively captures linear patterns in data, providing a valuable contrast to the more complex models in our evaluation.

Appendix D Full Results

Main Results

Tables 6 and 7 provide a detailed comparison of predictive models, including ARIMA, Logistic Regression, LSTM, Transformer, Informer, DLinear, and HMF, evaluated on the CH-OPBP and VitalDB datasets. The models were tested with sampling rates of 1 second and 3 seconds for the CH-OPBP dataset, and 1 second for the VitalDB dataset, across prediction scopes of 100, 200, and 300. Their performance was evaluated using key metrics such as Mean Squared Error (MSE), Mean Absolute Error (MAE), Area Under the Curve (AUC), Accuracy, and Recall.

In the analysis of the CH-OPBP dataset, as shown in Table 6, the HMF model consistently outperformed all other models across various prediction lengths and sampling rates. The HMF model achieved the lowest MSE and MAE values, demonstrating its superior ability to capture the intricate and non-stationary dynamics of intraoperative blood pressure trends. This contrasts with the ARIMA model, which performed relatively well at shorter prediction lengths with a longer sampling rate, but its performance significantly deteriorated as the prediction length increased, highlighting its limitations for longer-term forecasting. The HMF model

also demonstrated superior performance in terms of AUC, achieving the highest values across all conditions, further emphasizing its robustness in detecting IOH events.

Similarly, in the analysis of the VitalDB dataset, as presented in Table 7, the HMF model outperformed other models, particularly in terms of AUC and Recall. For instance, with a 3-second sampling rate and a shorter prediction length, the HMF model achieved notably higher AUC and Recall compared to other models. This performance highlights the HMF model’s effectiveness in scenarios involving complex temporal patterns and significant variability in blood pressure trends, characteristic of MAP series. In contrast, models like LSTM and Transformer, although competitive in some metrics, struggled with recall, often failing to capture the nuanced patterns necessary for accurate IOH prediction over longer sequences. Logistic Regression and ARIMA models exhibited substantial declines in performance across most metrics, particularly as the prediction length increased, reflecting their limitations in handling the intricate temporal dependencies present in MAP series.

Ablation Study

To better understand the contribution of each component within the HMF framework, an ablation study was conducted using the CH-OPBP dataset. This study specifically examined the impact of removing instance normalization and sequence decomposition on the model’s performance in predicting Mean Arterial Pressure (MAP) and detecting Intraoperative Hypotension (IOH) events.

Instance normalization plays a critical role in the HMF model by addressing the non-stationary nature of intraoperative MAP. As shown in Table 8, the complete HMF model, which includes instance normalization, consistently outperforms the variant without this component. The complete model achieves the lowest Mean Squared Error (MSE) and Mean Absolute Error (MAE) values, alongside the highest Area Under the Curve (AUC) and Recall across all prediction lengths. In contrast, removing instance normalization results in a marked increase in MSE and MAE, particularly on hypotensive data points, and a significant decline in AUC and Recall. These results indicate that instance normalization is crucial for maintaining the model’s precision and sensitivity. Without this component, the model struggles to manage the inherent variability in the data, leading to reduced accuracy in detecting IOH events.

Sequence decomposition is another vital component that enhances the HMF model’s ability to disentangle complex temporal dynamics within MAP. The ablation study reveals that excluding sequence decomposition leads to a noticeable decline in performance, particularly in terms of AUC and Recall. The complete model, which includes sequence decomposition, demonstrates superior performance across all metrics, achieving the highest scores for AUC and Recall. When sequence decomposition is removed, the model’s ability to capture underlying patterns and trends within the time series is significantly impaired, resulting in poorer performance. These findings highlight the importance of sequence decomposition in enhancing the model’s capability to accurately identify and predict IOH events.

²<https://github.com/blue-yonder/tsfresh>

Table 6: Performance Comparison of Different Methods Using The CH-OPBP Dataset.

Model	Sample(s)	Pred	MSE	MAE	AUC	Accuracy (%)	Recall (%)
Arima	1	300	97.1580	7.5501	0.6071	90.34	23.33
		600	118.0238	8.8539	0.6022	75.15	25.53
		900	175.6289	10.1539	0.5795	66.48	23.13
	3	100	26.9210	4.0537	0.6625	86.60	38.46
		200	155.1008	10.0347	0.5870	77.27	22.22
		300	156.7626	10.3933	0.5288	63.03	16.28
logistics	1	300	N/A	N/A	0.5000	86.06	0.00
		600	N/A	N/A	0.6777	62.13	81.90
		900	N/A	N/A	0.3386	35.96	23.39
	3	100	N/A	N/A	0.5977	79.84	32.50
		200	N/A	N/A	0.7002	72.00	65.18
		300	N/A	N/A	0.7342	75.01	65.79
LSTM	1	300	98.2363	7.9263	0.5660	90.65	14.57
		600	122.3699	9.4033	0.5000	73.49	0.00
		900	133.7677	9.9659	0.5226	64.47	5.18
	3	100	104.2937	8.9187	0.5000	90.51	0.00
		200	127.8037	10.0756	0.5000	73.48	0.00
		300	141.1666	10.6498	0.5000	62.94	0.00
Transformer	1	300	106.0975	8.2478	0.6194	89.99	27.32
		600	126.0585	9.6861	0.5804	75.94	19.94
		900	148.2355	10.2089	0.5758	67.32	20.04
	3	100	93.5870	7.4800	0.6328	89.51	30.91
		200	112.6674	9.0762	0.5406	75.06	9.34
		300	108.3092	8.4761	0.6177	70.22	29.11
Informer	1	300	102.4836	8.2318	0.5663	90.41	14.95
		600	92.3734	7.6706	0.6952	79.20	48.91
		900	116.2513	8.4248	0.6741	73.93	42.27
	3	100	104.9414	8.1057	0.6065	90.11	24.28
		200	108.3698	8.7226	0.5934	77.23	21.25
		300	119.7905	8.3365	0.6835	74.24	45.59
DLinear	1	300	107.2025	8.2388	0.5468	90.39	10.61
		600	127.4571	9.6158	0.5316	74.75	7.20
		900	142.3762	10.1150	0.5208	64.33	4.82
	3	100	106.1303	8.2176	0.5587	90.27	13.42
		200	123.7473	9.4676	0.5711	76.31	16.21
		300	141.7650	10.2002	0.5271	64.72	6.30
HMF	1	300	73.7196	6.8555	0.7702	76.48	77.70
		600	89.8372	7.6161	0.7230	75.30	65.91
		900	116.2464	8.2751	0.7125	74.08	60.33
	3	100	77.0390	6.8708	0.7801	77.72	78.38
		200	88.6844	7.4293	0.7245	75.32	66.34
		300	93.7548	7.5482	0.7194	73.55	65.68

The results of this ablation study clearly demonstrate that both instance normalization and sequence decomposition are integral to the HMF model’s success in predicting MAP and detecting IOH events. The inclusion of these components allows the HMF model to effectively manage the complexities of intraoperative MAP, ensuring high predictive accuracy and reliability. Removing either component leads to a significant reduction in performance, underscoring their essential roles in the overall framework.

Visualization Results

Our analysis of the CH-OPBP dataset, using a 15-minute context window and a 3-second sampling rate, consistently demonstrates the superiority of the HMF framework in predicting IOH events across various prediction horizons. We evaluated the performance of different models with prediction lengths of 100, 200, and 300, as illustrated in Fig.7, Fig.8, and Fig. 9, respectively. The results consistently indicate that HMF excels in accurately detecting the onset of MAP decline, thereby effectively identifying IOH events.

In contrast, alternative models exhibit significant difficul-

Table 7: Performance Comparison of Different Methods Using The VitalDB Dataset.

Model	Sample(s)	Pred	MSE	MAE	AUC	Accuracy(%)	Recall(%)
Arima	3	100	193.3889	10.7640	0.5397	83.10	10.42
		200	268.3629	13.7636	0.5073	60.27	5.48
		300	310.3584	14.8105	0.5280	53.20	9.68
logistics	3	100	N/A	N/A	0.5094	78.52	2.11
		200	N/A	N/A	0.5877	61.80	37.50
		300	N/A	N/A	0.5814	58.41	60.80
LSTM	3	100	157.8527	10.6642	0.5000	84.35	0.00
		200	204.0663	12.3266	0.5000	61.35	0.00
		300	204.2178	12.5930	0.5000	48.58	0.00
Transformer	3	100	162.8149	10.6928	0.5022	84.36	0.54
		200	162.6087	10.8778	0.5006	61.40	0.13
		300	150.6858	10.4997	0.5091	49.50	2.12
Informer	3	100	164.9233	11.0281	0.5000	84.35	0.00
		200	152.0211	10.7310	0.5000	61.35	0.00
		300	159.4176	10.9371	0.5008	48.66	0.16
DLinear	3	100	173.4594	11.1419	0.5097	84.33	2.41
		200	175.6332	11.4898	0.5077	61.85	1.97
		300	176.2505	11.8588	0.5049	49.08	1.19
HMF	3	100	149.5450	8.7662	0.6819	78.29	53.50
		200	165.2017	9.3708	0.6370	68.01	44.74
		300	182.5259	10.0166	0.6215	61.50	39.38

Table 8: Performance Comparison of Ablation Study Using The CH-OPBP Dataset.

Model	Sample(s)	Pred	MSE	MAE	AUC	Accuracy(%)	Recall(%)
HMF	3	100	77.0390	6.8708	0.7801	77.72	78.38
		200	88.6844	7.4293	0.7245	75.32	66.34
		300	93.7548	7.5482	0.7194	73.55	65.68
w/o instance normalization	3	100	94.9945	7.6259	0.6295	90.02	29.55
		200	107.6521	8.6942	0.5800	76.63	18.34
		300	118.2548	9.1814	0.5578	66.51	14.29
w/o time series decomposition	3	100	98.1400	7.8539	0.5759	90.26	17.27
		200	106.0578	8.6880	0.5729	76.18	17.08
		300	112.9715	8.9473	0.5763	67.85	18.15

ties in capturing the downward trend in MAP, resulting in poorer classification performance. This underperformance underscores the limitations of these models, particularly in scenarios involving rapid fluctuations in MAP. The superior performance of HMF across all prediction lengths can be attributed to its enhanced capacity to learn and generalize from the dataset, even under challenging conditions. This robustness and accuracy highlight the effectiveness of our approach, establishing HMF as a reliable tool for predicting IOH events in dynamic clinical settings.

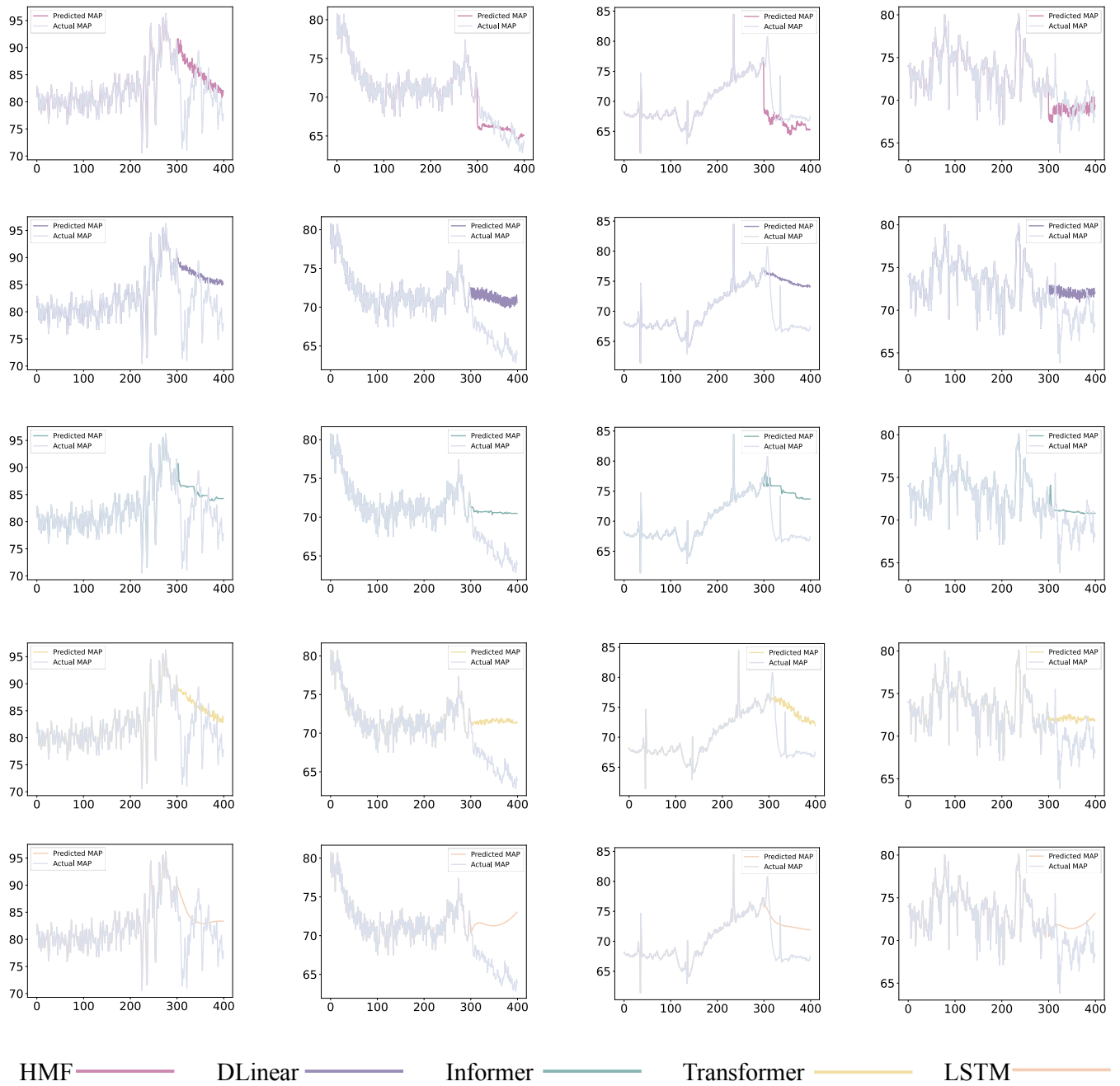


Figure 7: Visual Results of Various Models for Context window length of 300 and Predicted Scope Length of 100.

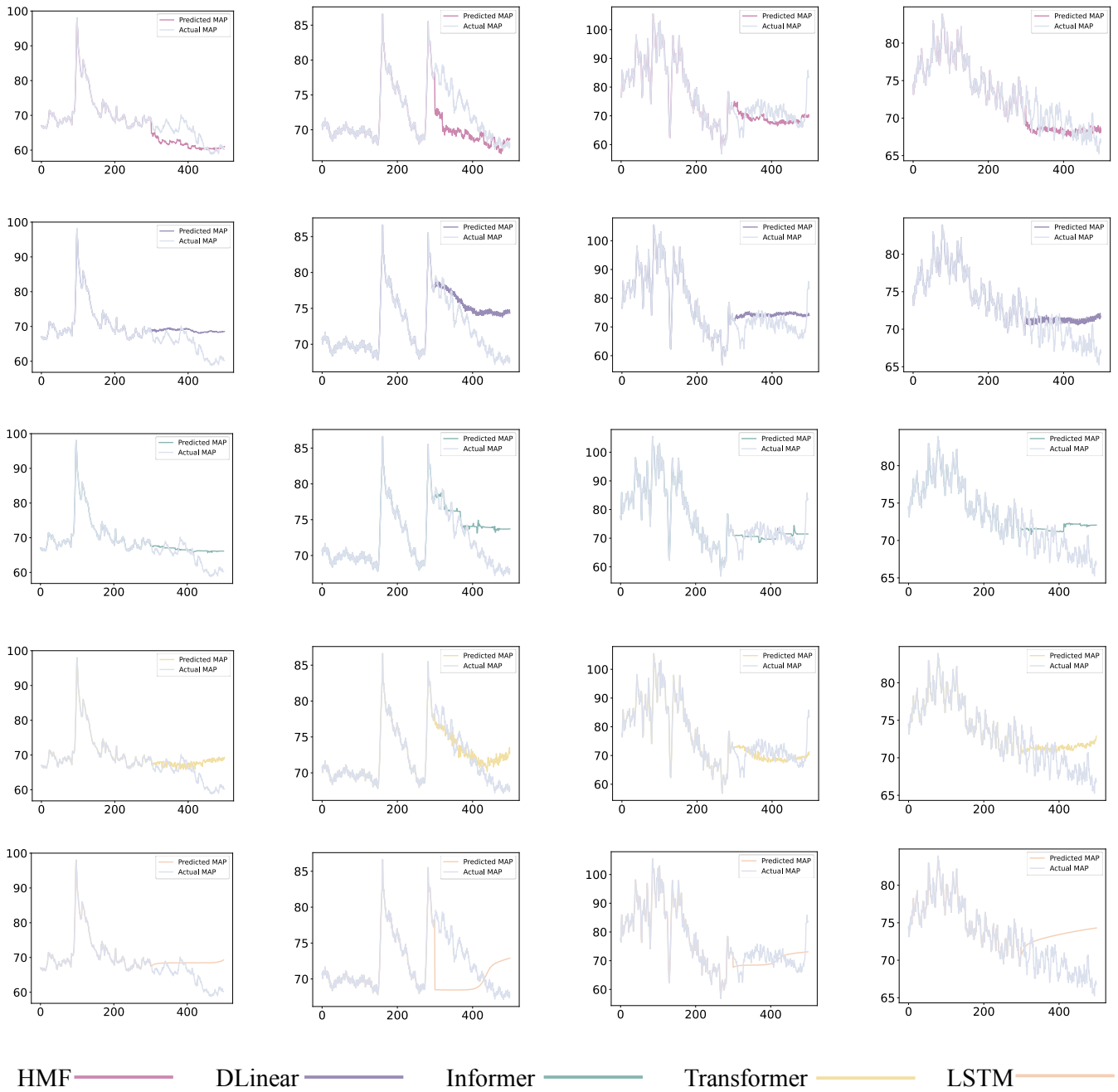


Figure 8: Visual Results of Various Models for Context window length of 300 and Predicted Scope Length of 200.

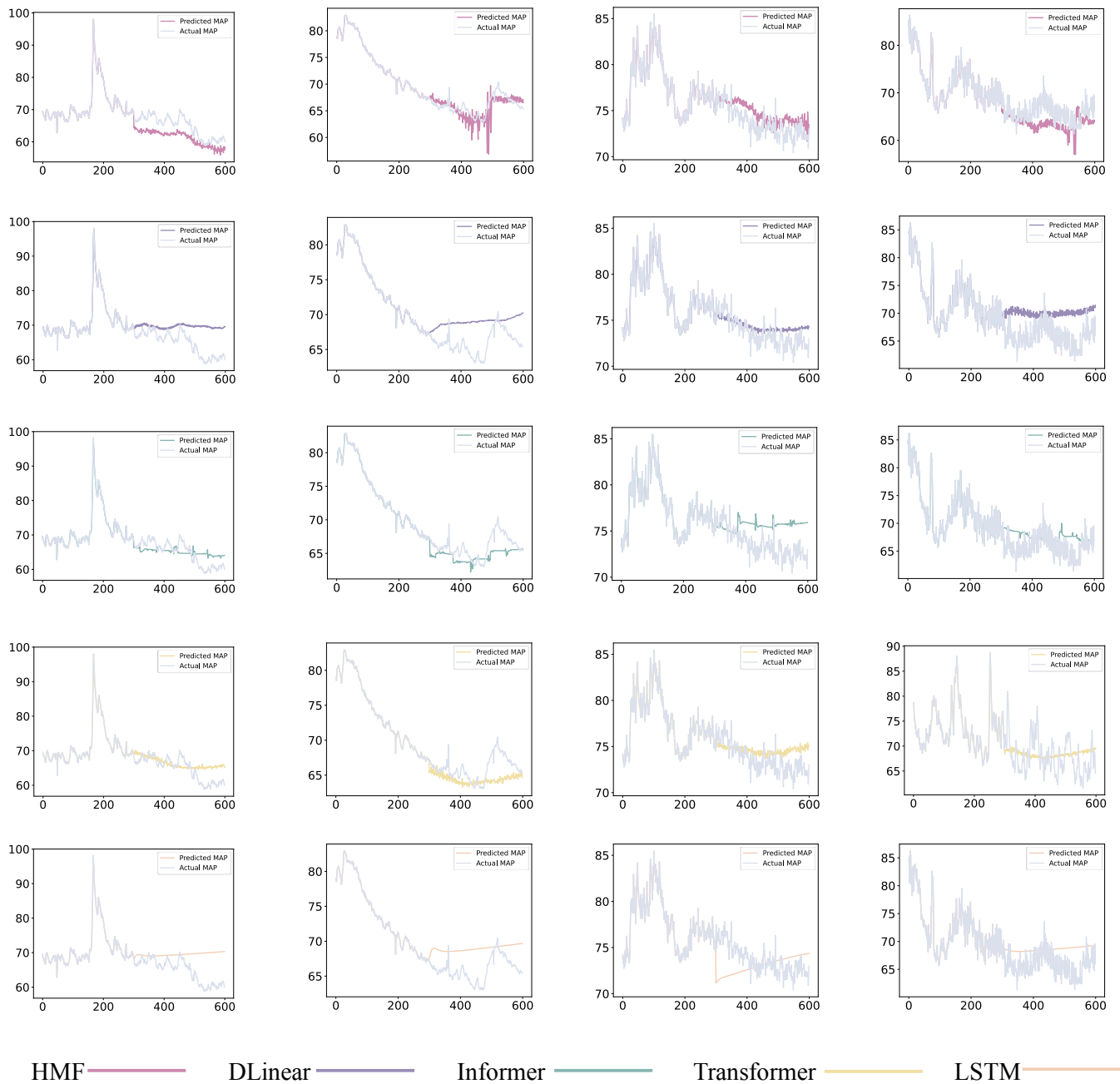


Figure 9: Visual Results of Various Models for Context window length of 300 and Predicted Scope Length of 300.